

# FEASIBILITY OF PRODUCING NANO STRUCTURED METALLIC AND NON-METALLIC COATINGS ON Al SUBSTRATE USING MECHANICAL COATING ROUTE

A. Yazdani\* and A. R. Zakeri

\* arash\_yazdani@metaleng.iust.ac.ir

Received: February 2015

Accepted: May 2015

School of Metallurgy and Materials Engineering, Iran University of Science & Technology, Tehran , Iran.

**Abstract:** In this paper, the possibility of mechanical coating of aluminum with either Ni or SiC using planetary ball mill was studied. The Al substrate was fixed inside of the vial lid of a planetary ball mill filled with milling balls and starting powder. The phase analysis and crystallite size measurement of the coatings were carried out using X-ray diffraction (XRD) method. Scanning electron microscope (SEM) was employed to study the coating/substrate interface and coating thickness. Hardness and wear resistance of coatings were also measured. The results indicated that all coatings have relatively uniform thickness. SiC coating shows poor compaction and adhesion to the Al, while nano-structured Ni coating is well-bonded to the substrate. Moreover, Ni coating showed higher hardness and wear resistance compared to SiC coating. It was found that the balls collision will result in the grain refinement of the coating as well as Al substrate. Mechanically deposited Ni coating shows higher hardness value compared to those obtained by conventional methods. This has been related to the induced grain refinement phenomenon.

**Keywords:** Mechanical coating, planetary ball mill, Hardness, Ni and SiC coatings.

## 1. INTRODUCTION

In most engineering applications, the failure of components begins from the surface. This clearly shows the importance of optimization of the properties and structure of the surface layer in order to increase the life time of tools. Mechanical alloying (MA) and surface mechanical attrition treatment (SMAT) processes have been successfully combined to mechanical coating (MC) of metallic substrates. In MC process, mechanical activation of sample surfaces which could be easily fulfilled at ambient temperature and atmospheric pressure enhances the bonding between coating and substrate [1, 2]. Researches in the field of MC could be classified from different viewpoints: (i) position of the substrate, (ii) coating material and (iii) used equipments. Milling balls [3], inner wall of the container [4], plate inside the powder mixture [5] top [6] and end plate of the vibration chamber [1] have been investigated as the position of the substrate. Interestingly, large varieties of coatings (ceramic, metallic and inter metallic) such as Ti-Al [7], Ni-Cu [8], Ni-Al [9], Zr-Ti [10], Ti-Cr [4], Fe-Al [5], TiN [11] and etc.,

have been mechanically deposited. In the case of equipments, several set-ups like mechano-reactor [12] and ultrasonic [11] -based vibration chamber, SPEX 8000 mixer mill [10] and planetary ball mill [5] have been employed.

It is well known that during mechanical milling process powder, balls and milling vial show two main behaviors: collision and rubbing which will lead to revealing the impact energy and friction. According to the simulation results, two main types of movement have been identified for powder and balls: agitation and ball thrown. Agitation movements happen in the vibratory ball mills and shakers swinging in vertical or horizontal or combinatorial directions (e. g. in SPEX mill). In these cases, the balls, relevant end/top of vial and the sample in the mixture are strongly prone to be coated with powder. The second type of motion, ball thrown, is commonly seen in conventional and planetary ball mills. In this case, milling balls, inner wall of vial and the sample in the mixture could be easily coated during the milling process [13]. Although there is no evidence on the collision of ball onto the vial lid in the planetary ball mill, it is possible to provide such condition using many small balls.

Hence, in this research, we aim to study of feasibility of deposition metallic (Ni) and ceramic (SiC) coatings on the Al substrate fixed at the vial lid of a planetary ball mill. In the next stage, the microstructure and mechanical properties of produced coatings will be examined.

## 2. EXPERIMENTAL PROCEDURE

Commercial pure aluminum was used as substrate. Aluminum plate with 2 mm thickness was fixed inside of the vial lid with 5 cm diameter. A schematic presentation of used set up is shown in Fig. 1. As-received Ni and SiC powders (>99.5%,  $\sim 10\mu$ ) were used as starting raw materials. The mechanical coating process was carried out in a home-made planetary ball mill at constant sun-wheel rotation speed of 300 rpm for 5 hours. For all coating treatments, half of the vial was filled with equal number of 6 and 8 mm diameter bearing steel balls. The ball-to-powder weight ratio for all coating trials was 30.

The phase composition of the coatings was studied by X-ray diffraction (XRD) analysis using a PANalytical, X'Pert Pro MPD with a Cu  $K\alpha_1:K\alpha_2$  radiation ( $\lambda = 1.5418 \text{ \AA}$ ). For Rietveld refinement the Topas program was used. The

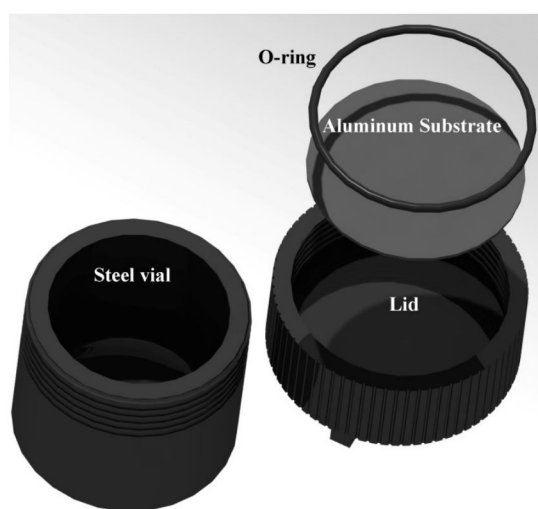


**Fig. 1.** A schematic illustration of the set up used for the mechanical coating.

surface morphology and cross-sectional microstructure of the coatings were studied using a VEGA II TESCAN scanning electron microscope (SEM) equipped with energy dispersive X-ray spectroscopy (EDS) system. Microhardness measurements were carried out using an MHV-1000Z digital Micro Vickers hardness tester at a load of 50 g and a dwell time of 15 s. The microhardness values were the average of eight measurements. Dry sliding pin-on-disc wear tests were performed in a laboratory atmosphere at 30-40% relative humidity and the temperature around 25°C. The normal load of 10 N was used in the wear tests and the rotation speed was  $0.2 \text{ ms}^{-1}$  with a radius of 11 mm for 300 m sliding. The material of the pin was AISI 52100 hardened steel with the hardness of 55 HRC. The weight of each specimen was measured using an electronic balance having a precision of 0.1 mg, before and after each wear test.

## 3. RESULTS AND DISCUSSIONS

In order to deep understanding of balls movement in the milling vial, a very simple set of experiments was carried out. Play clay was adhered on to the Al substrate. Then coated substrate was wrapped in a plastic bag. Wrapped and not wrapped plates were fixed into the vial lid. Half of the milling vial was filled with 6 and 8 mm balls without powder. Milling was carried out for 5 minutes. After the milling, photos of the clay surface were taken (Figs. 2a and b).

Fig. 2a shows that balls movement on the surface of wrapped play clay has left visible shear marks behind which are in fact the path way of balls. These shear marks could be seen all over play clay especially at the edge of clay created by the strong centrifugal forces which are applied by the movement of balls. In the case of unwrapped clay (Fig. 2b), it is seen that a row of balls have been stuck in the clay. Meanwhile, some rings are observed on the surface of sample. Shearing force causes the play clay to flow and its accumulation at the contact points of ball rows (forming the circular rings) and the central point of clay (forming the protruded region). Centrifugal force provides different orientations for balls with different sizes.

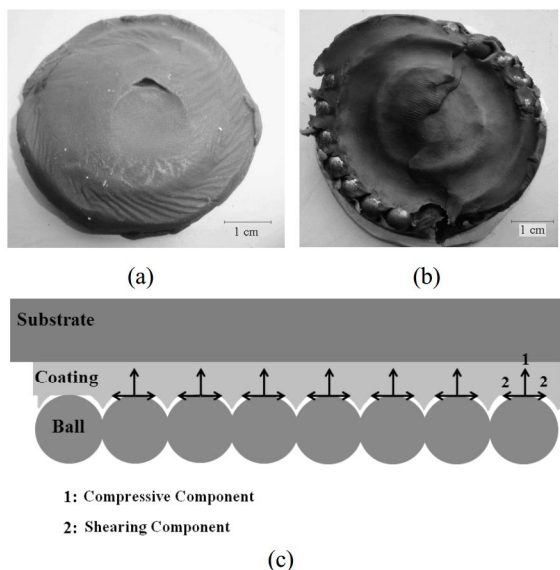


**Fig. 2.** Photographs of (a) wrapped play clay with a plastic bag (b) not wrapped play clay. (c) A schematic illustration of materials accumulation phenomenon on the surface of coating by ball collision.

As a result, larger balls, due to their greater mass, are pushed toward the edge of substrate by smaller balls. However, according to Fig. 2b it is seen that smaller balls have been stuck in the clay layer. It seems that the ball collisions cause a two-components force on the surface of substrate: (i) compressive component which consolidates the coating particles or hammers them into the substrate, (ii) shearing component which leads to the plastic flow (if possible) of the coating. According to Fig. 2b, shearing component of collision force of each ball pushes out the coating materials toward the neighbouring ball. This plastic flow occurs around every two neighbouring balls leading to the accumulation of the coating materials near the contact points of balls on the substrate surface. A schematic illustration of this phenomenon is shown in Fig. 2c.

In the macroscopic scale, the shearing force applied by the balls collision along with a size-gradient orientation of balls from the edge to the central point of coated substrate, lead to the formation of circular rings on the surface of Ni coating (Fig. 3a). SiC coating (Fig. 3b) is made of SiC particles which are rearranged by each ball

collision leading to the formation of coating with uniform surface appearance without any circular rings. In other words, prolonged coating times and balls collision lead to the particles sliding, rearranging and restacking with a high degree of voidage.

According to the cross sectional SEM image of pure Ni coating (Fig. 4a), it is seen that the Ni particles are hammered into the Al substrate. Moreover, it is clear that Ni particles have been cold welded to each other and pressed into the substrate. Nickel particles are observed in the regions several tens micron deep in the substrate (Fig. 4b). Most probably, at the initial stage of the coating process, the Ni particles adhere to the Al. Continuous ball collisions pushes adhered Ni particles deep inside the Al substrate as well as adheres fresh Ni particles on to the cold welded Ni ones.

Fig. 4c shows the cross sectional image of SiC coating. It is seen that SiC layer is mechanically adhered to the substrate. Energy transferred from balls collision leads to the plastic deformation of the aluminum substrate. Consequently, the

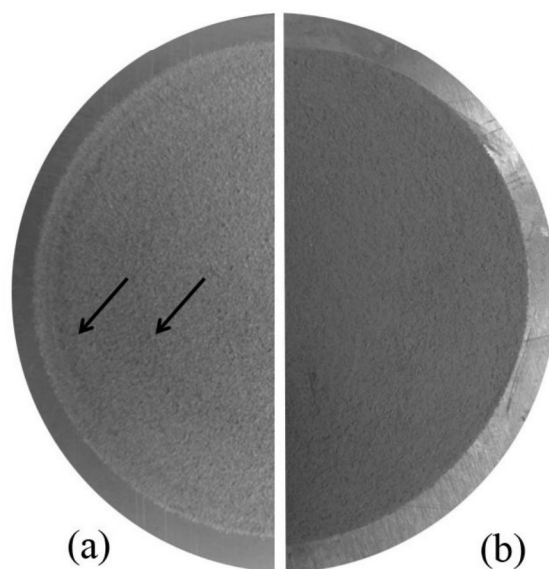


**Fig. 3.** Photographs of (a) Ni and (b) SiC coatings. Circular rings are marked with black arrows. The diameter of plate is 45 mm.

surface roughness of substrate increases leading to the formation of protruded region which facilitates the mechanical bonding between SiC coating and substrate.

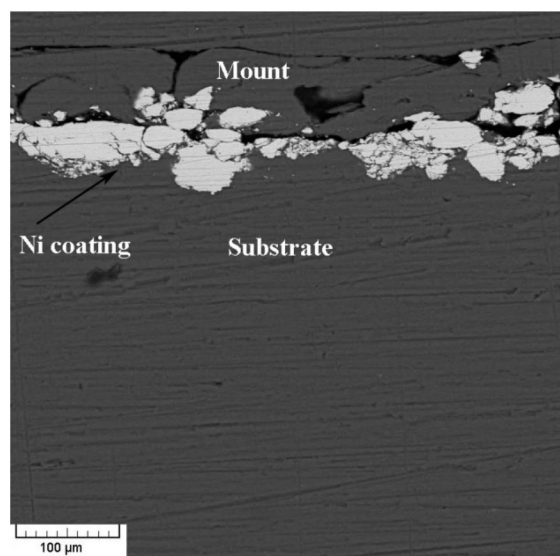
SiC coating is consisted of SiC particles which have been partially compacted together. Relatively high density of pores (black areas) is observed (Figs. 4d and e). Moreover, it is clearly seen that the coating is not properly bonded to the substrate. Cracks are easily seen in the coating/substrate interface and even through the coating (Fig. 4d).

It was mentioned previously that balls collision pushes the Ni particles to the contact point between two neighbouring balls leading to the materials accumulation and formation of circular ring on the surface of Ni coating. On the other hand, for SiC coating, particles sliding and rearranging occurs and the final coating features even appearance. In the microscopic scale, it is seen that SiC coating has relatively even thickness compared to Ni one which is in good agreement with macroscopic observations.

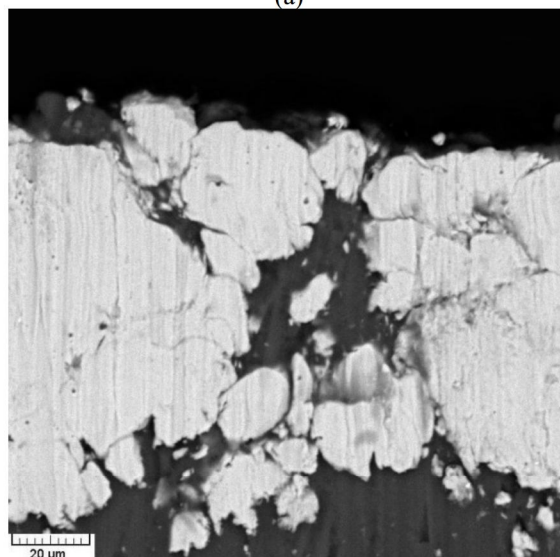
The micro hardness of SiC and Ni coatings is about  $71.56 \pm 10.20$  HV0.05 and  $442.09 \pm 19.82$  HV0.05, respectively. Very low hardness of SiC coating is due to the poor compaction of SiC particles and high degree of porosity in the coating. On the other hand, the hardness of Ni coating is relatively higher than that of Ni coatings deposited using conventional methods (e. g. electro or electroless deposition). Mainly, hardness values between 200-300 Vickers have been reported for Ni coatings [14-16]. Balls collision results in the surface hardening by grain refinement in the coating, especially surface layer. Hence, it is expected to obtain higher hardness value for mechanically deposited Ni coating compared to other known methods.

Fig. 5 shows the XRD patterns of fabricated coatings. Table 1 shows the results of the Rietveld refinements of the X-ray patterns corresponding to Ni and SiC coatings.

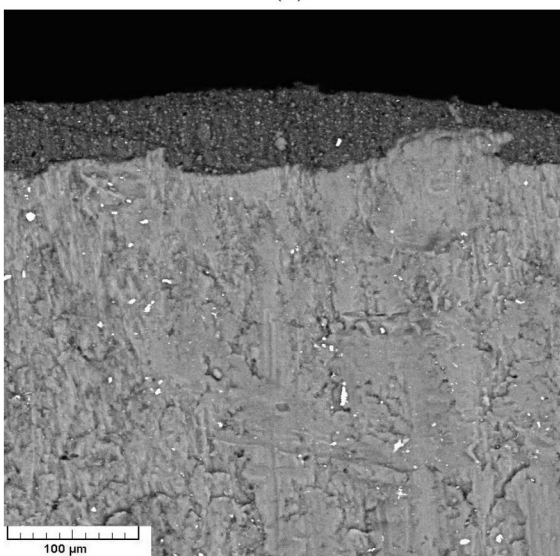
As indicated in this table, Ni coating is consisted of cold welded Ni particles with crystallite size of 45.4 nm accompanied by 8.71 wt% of amorphous phase. Amorphous Ni phase is formed due to the increase of structural defects (such as dislocation blocks and stacking faults)



(a)



(b)



(c)

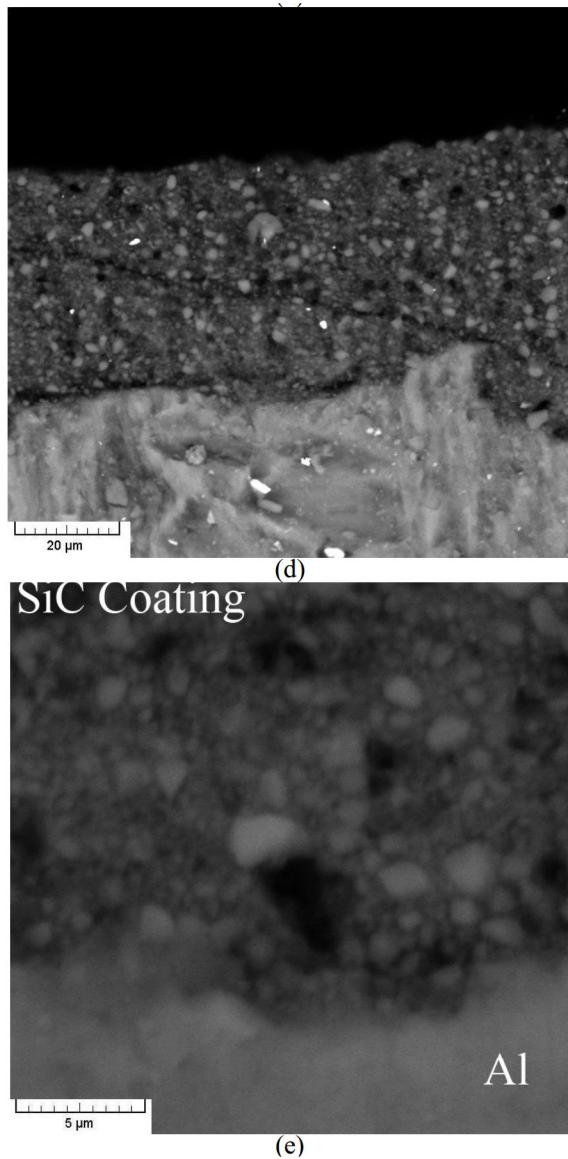


Fig. 4. Cross sectional SEM image of (a, b) Ni and (c, d, e) SiC coatings at different magnifications.

induced by balls collision. In the case of SiC coating, 14.76 wt% of aluminum was detected. Abrasive SiC particles abrade the aluminum substrate during the coating process. As a result, spalled aluminum particles will be blended with the initial SiC powder and re-deposited on the substrate. Interestingly, it is seen that the crystallite size of Al substrate is smaller than that of SiC coating. One can conclude that energy of the flying balls transfers to the coating material as well as substrate. Consequently, grain refinement and surface hardening will occur in the coating

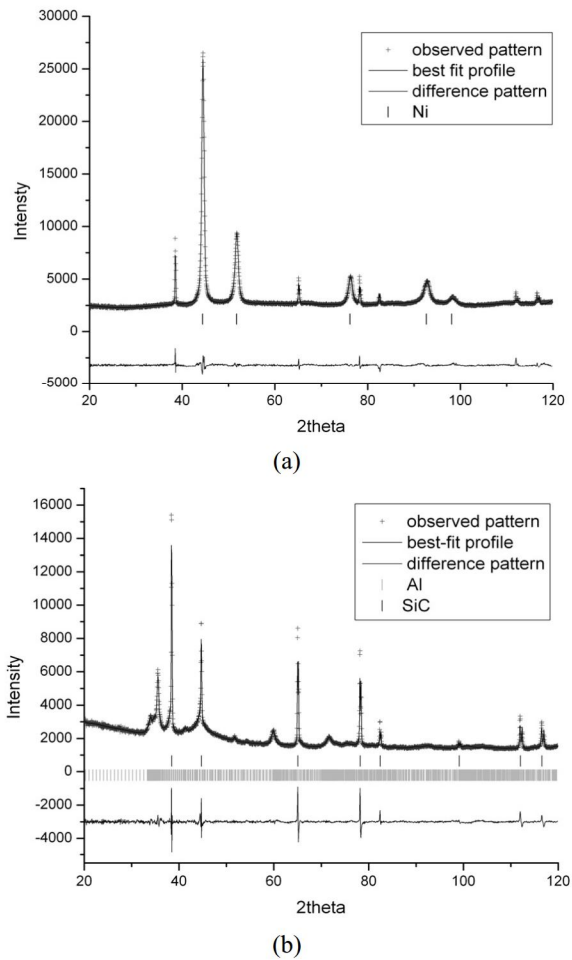


Fig. 5. XRD patterns of (a) Ni and (b) SiC coatings.

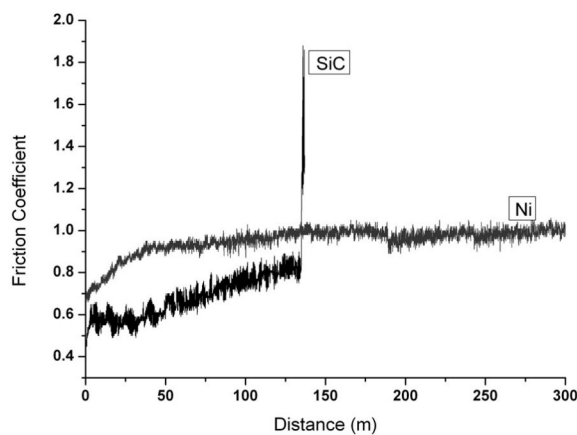
layer and region near the surface of substrate.

Fig. 6 represents the friction coefficients and wear rate of the Ni and SiC coatings tested to a 300-m sliding distance.

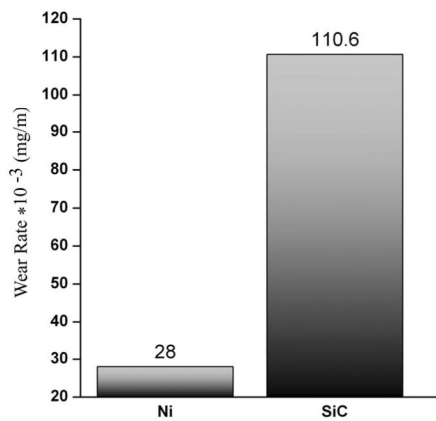
According to Fig. 6a, it is seen that Ni coating has a relatively constant friction coefficient of 0.95. In the case of SiC coating, friction coefficient is low at the beginning of wear process (starting 50 m). After that, the friction coefficient gradually increases which is due to the fracture of coating. Further wear results in the complete delamination of the coating from the substrate. This is in good agreement with the previous statement about the poor compaction and bonding of this coating. Wear rate of produced coatings are shown in Fig. 6b. It is seen

**Table1.** Crystallite size and weight percent of identified phases in the produced coatings along with the Rwp and GOF of the Rietveld refinement

Sample	Cubic Ni		Trigonal SiC		Cubic Al		Amorphous phase		R <sub>wp</sub>	GOF
	D (nm)	Wt.%	D (nm)	Wt.%	D (nm)	Wt.%	D (nm)	Wt.%		
Ni Coating	D (nm)	45.4	D (nm)	-	D (nm)	-	D (nm)	-	0.02949	1.622
	Wt.%	91.29	Wt.%	-	Wt.%	-	Wt.%	8.71		
SiC Coating	D (nm)	-	D (nm)	168.9	D (nm)	148.59	D (nm)	-	0.04315	1.954
	Wt.%	-	Wt.%	85.24	Wt.%	14.76	Wt.%	-		



(a)



(b)

**Fig. 6.** (a) Friction coefficient and (b) wear rate of Ni and SiC coatings.

that wear rate of SiC coating is significantly higher compared to that of Ni coating.

In order to detail investigation on the wear mechanism, the wear tracks were observed by

SEM on top surface (Fig. 7). It is clearly seen that the width of wear track on the SiC coating is greater compared to that of Ni coating confirming higher wear resistance of Ni coating. Moreover, adhesive wear seems to be the main wear mechanism for both coatings. This type of wear is characterized by the flow of coating material in a wavy form and formation of deep grooves caused by the ploughing of hard asperities on the steel pin and work-hardened transfer particles. Signs of plastic deformation on the surface of Ni coating are contributed to the deformation of Ni particles. On the other hand, adhesive wear of SiC coating is related to the plastic deformation of Al substrate. As it was mentioned previously, SiC coating has poor compaction and bonding to the substrate. As a result, SiC coating cannot withstand the stress applied during the wear test.

#### 4. CONCLUSION

In this research, Al substrate fixed at the top lid of a planetary ball mill was successfully coated with Ni and SiC. A relatively uniform coating, either Ni or SiC, was produced using mechanical coating technique. SiC coating showed low compaction degree resulted in poor compaction, bonding to the substrate, lower hardness and wear resistance. On the other hand, Ni coating was well compacted and bonded to the Al without any visible defect in the coating/substrate interface. Higher hardness of mechanically produced Ni coating, compared to those deposited by electro or electroless deposition methods, was attributed to the grain refinement induced by ball collisions.

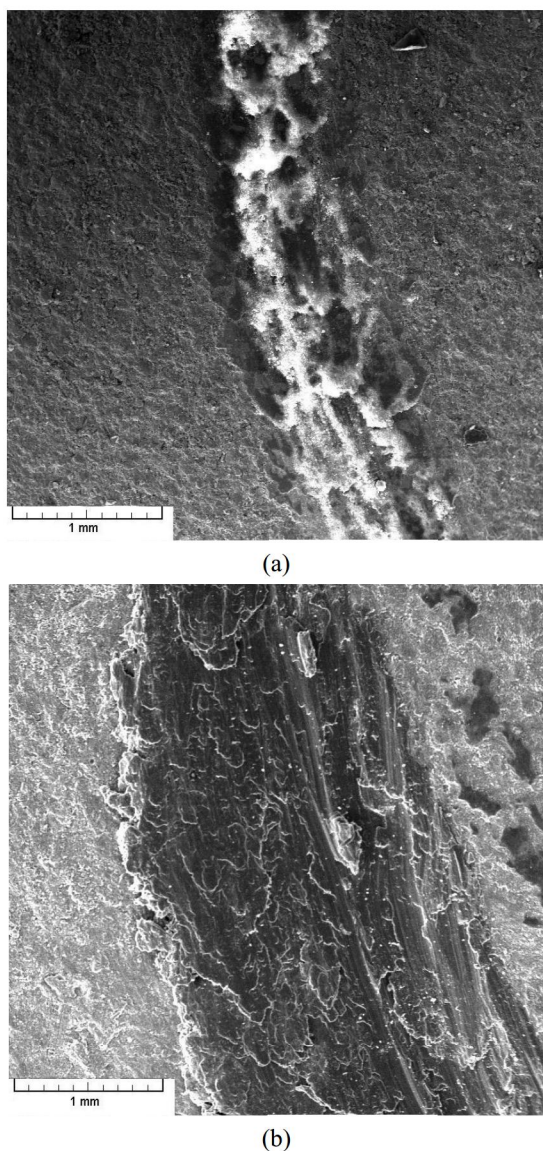


**Fig. 7.** SEM micrographs of worn surfaces of (a) Ni and (b) SiC coatings.

## REFERENCES

- Révész, Á., Takacs, L., "Alloying and amorphization by surface mechanical treatment", *Materials Science Forum*, 659 (2010) 239–244.
- Komarov, S. V., Romankov, S. E., Hayashi, N., Kasai, E., "Nanostructured coatings produced by a novel ultrasonic-assisted method: Coating characterisation and formation mechanism", *Surf Coat Technol* 2010; 204: 2215–2222.
- Hao, L., Lu, Y., Sato, H., Asanuma, H., "Fabrication of zinc coatings on alumina balls from zinc powder by mechanical coating technique and the process analysis", *Powder Technol*, 228 (2012) 377–384.
- Li, B., Ding, R., Shen, Y., Hu, Y., Guo, Y., "Preparation of Ti–Cr and Ti–Cu flame-retardant coatings on Ti–6Al–4V using a high-energy mechanical alloying method: A preliminary research", *Mater Design*, 35 (2012) 25–36.
- Canakci, A., Erdemir, F., Varol, T., Ozkaya, S., "Formation of Fe–Al intermetallic coating on low-carbon steel by a novel mechanical alloying technique", *Powder Technol*, 247 (2013)24-29.
- Romankov, S., Hayasaka, Y., Shchetinin, I. V., Yoon, J. M., Komarov, S. V., "Fabrication of Cu–SiC surface composite under ball collisions", *Appl Surf Sci.*, 257 (2011) 5032–5036.
- Romankov, S., Kaloshkin, S. D., Hayasaka, Y., Hayashi, N., Kasai, E., Komarov, S. V., "Effect of process parameters on the formation of Ti–Al coatings fabricated by mechanical milling", *J Alloys Compd.*, 484 (2009) 665–673.
- Farahbakhsh, I., Zakeri, A., Manikandan, P., Hokamoto, K., "Evaluation of Nanostructured coating layers formed on Ni balls during mechanical alloying of Cu powder", *Appl Surf Sci.*, 257 (2011) 2830–2837.
- Pouriamanesh, R., Vahdati-Khaki, J., Mohammadi, Q., "Coating of Al substrate by metallic Ni through mechanical alloying", *J Alloys Compd*, 488 (2009) 430–436.
- Révész, A., Takacs, L., "Coating a Cu plate with a Zr–Ti powder mixture using surface mechanical attrition treatment", *Surf Coat Technol.*, 203 (2009) 3026–3031.
- Romankov, S., Hayasaka, Y., Hayashi, N., Kasai, E., Komarov, S., "Effect of annealing treatment on the structure and properties of the nanograined TiN coatings produced by ultrasonic-based coating process", *J Alloys Compd.*, 495 (2010) 625–628.
- Romankov, S., Hayasaka, Y., Kasai, E., Yoon, J. M., "Fabrication of nanostructured Mo coatings on Al and Ti substrates by ball impact cladding", *Surf Coat Technol.*, 205 (2010)

- 2313–2321.
13. Budin, S., Almanar, I. P., Kamaruddin, S., Che Maideen, N., Zulkifli, A. H., “Modeling of vial and ball motions for an effective mechanical milling process”, *J Mater Process Technol.* 209 (209) 4312–4319.
  14. Zhou, Y., Zhang, H., Qian, B., “Friction and wear properties of the co-deposited Ni–SiC nanocomposite coating”, *Appl Surf Sci.*, 253 (2007) 8335–8339.
  15. Gül, H., Kılıç, F., Uysal, M., Aslan, S., Alp, A., Akbulut, H., “Effect of particle concentration on the structure and tribological properties of submicron particle SiC reinforced Ni metal matrix composite (MMC) coatings produced by electrodeposition”, *Appl Surf Sci.*, 258 (2012) 4260–4267.
  16. Narasimman, P., Pushpavanam, M., Periasamy, V. M., “Synthesis, characterization and comparison of sediment electro-codeposited nickel–micro and nano SiC composites”, *Appl Surf Sci.*, 258 (2011) 590–598.